Inorganic Chemistry

Article

pubs.acs.org/IC

Photochromic Properties of Polyoxotungstates with Grafted Spiropyran Molecules

Arnaud Parrot,[†,‡] Guillaume Izzet,*[,†] Lise-Marie Chamoreau,[†] Anna Proust,[†] Olivier Oms,[‡] Anne Dolbecq,[‡] Khadija Hakouk,[§] Houda El Bekkachi,[§] Philippe Deniard,[§] Rémi Dessapt,*[,§] and Pierre Mialane*[,‡]

[†]Institut Parisien de Chimie Moléculaire, IPCM, UMR CNRS 7201, Université Pierre et Marie Curie, UPMC Univ Paris 06, 4 Place Jussieu, Case 42, F-75005 Paris, France

[‡]Institut Lavoisier de Versailles, UMR 8180, Université de Versailles Saint-Quentin en Yvelines, 45 Avenue des Etats-Unis, F-78035 Versailles cedex, France

[§]Institut des Matériaux Jean Rouxel, Université de Nantes, CNRS, 2 rue de la Houssinière, BP 32229, 44322 Nantes cedex, France

Supporting Information

ABSTRACT: The first systems associating in a single molecule polyoxotungstates (POTs) and photochromic organic groups have been elaborated. Using the $(TBA)_4[PW_{11}O_{39}\{Sn(C_6H_4I)\}]$ precursor, two hybrid organic−inorganic species where a spiropyran derivative (SP) has been covalently grafted onto a $\{PW_{11}Sn\}$ fragment via a Sonogashira coupling have been successfully obtained. Alternatively, a complex containing a silicotungstate $\{PW_{11}Si_2\}$ unit connected to two spiropyran entities has been characterized. The purity of these species has been assessed using several techniques, including ^1H and ^{31}P NMR spectroscopy, mass spectrometry, and electrochemical measurements. The optical properties of the hybrid materials have been investigated both in solution and in the solid state. These studies reveal that the grafting of SPs onto POTs does not significantly alter the photochromic behavior of the organic chromophore in solution. In contrast, these novel hybrid SP−POT materials display highly effective solid-state photochromism from neutral SP molecules initially nonphotochromic in the crystalline state. The photoresponses of the SP−POT systems in the solid state strongly depend on the nature and the number of grafted SP groups.

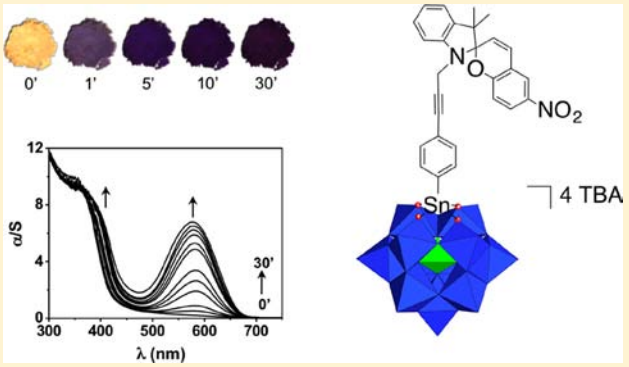

1. INTRODUCTION

Photochromic molecules display reversible transformations induced in one or both directions by electromagnetic radiations between two states having different absorption spectra.[1] Among the numerous organic compounds that possess such behavior, the class of spiropyran (SP) molecules has probably been the most widely studied these last 50 years, because of their high optical performances and their synthetic accessibility.[2] In their closed form (CS), the colorless SP molecules contain a C_{spiro}−O bond that can be cleaved under near-UV irradiation, leading to a zwitterionic merocyanin (MC) isomer. This latter, compared to the CS form, strongly absorbs in the visible region. The CS form can then be regenerated under thermal activation or via a photochemical pathway. For a huge majority of SP molecules, even low power UV irradiations can induce noticeable CS → MC isomerization in solution. In strong contrast, very few spiropyrans exhibit such transformation in the solid state and in ambient conditions.[3] Nonetheless, the elaboration of relevant solid-state photochromic materials is essential to develop effective photochromic devices in view of potential technological and marketable applications, which include smart windows, multicolor smart painting, UV sensors, cosmetics, optical switches, and 3D high-density optical data storage.[4] Fortunately, it has been shown that the elaboration of hybrid organic−inorganic materials based on photochromic organic molecules may overcome this problem.[5] In particular, sol−gel methods have been developed that enable formation of spiropyran-based solid-state photochromic materials.[6] It has also been shown that the inclusion of an SP in metal organic frameworks can strongly stabilize the MC form and can even lead to an antidromic reversible photochromic behavior.[7] Also, besides these examples where SP molecules are physically embedded into the cavities of a (meso)porous soft material or a crystalline coordination network, the covalent connection of SP chromophores to matrixes has also been made. We can especially note that SPs have been grafted on polymers.[8] In addition, SP molecules have been connected to coordination complexes, as exemplified by the characterization of an SP−porphyrin compound.[9] Nonetheless, the optical properties of

Received: June 5, 2013
Published: September 19, 2013

dx.doi.org/10.1021/ic401380a | Inorg. Chem. 2013, 52, 11156−11163

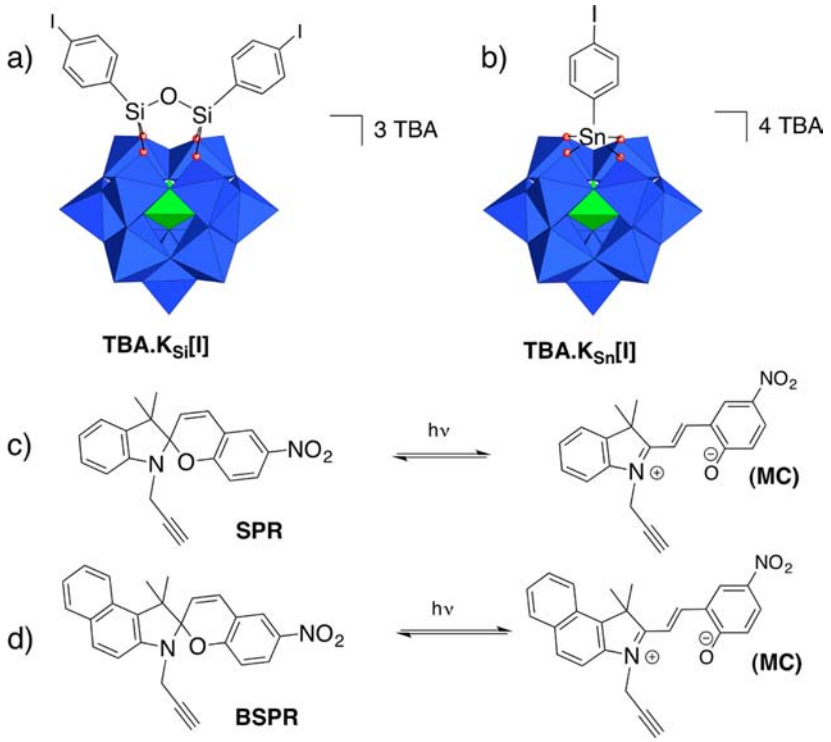

Figure 1. Representation of (a, b) the two POT precursors and of (c, d) the two spiropyran molecules used in this study and the SP → MC isomerization process.

this species have not been investigated in the solid state. Recently, we have initiated a study devoted to the elaboration of hybrid materials, displaying dual photochromic and electrochromic behaviors built from the association of polyoxometalates (POMs), a class of molecular oxides that exhibits an enormous diversity of structures and properties,[10] with spiropyran molecules. After the characterization of supramolecular materials where cationic SP$^+$ act as counterions for POM species,[11] we have successfully performed the covalent grafting of neutral SP molecules onto the polyoxomolybdate Anderson platform $\{MnMo_6O_{18}\}$.[12] If these compounds present solid-state photochromism properties due to a highly effective CS → MC isomerization, the influence of the POM on the photochromic performances of the hybrid materials was mostly limited to the kinetics of photoresponses since the spiropyran precursor was itself photoactive in the solid state. To clearly evidence a potential beneficial role of the POM fragment on the photochromic properties of connected SP molecules, it is necessary to elaborate covalent SP−POM dyads incorporating spiropyran units initially nonphotoactive in the solid state. Herein, we report the first examples of materials where such SP groups are connected to POM platforms. Because of their versatilities, and the well-established synthetic tools that allow their controlled covalent functionalization,[13] polyoxotungstates (POTs) have been considered as inorganic supports. Three compounds, differing by the nature of the POT (stannotungstate vs silicotungstate), resulting in different numbers of grafted SPs (one vs two) and different electron acceptor characters, and by the nature of the SP (spiropyran vs benzospiropyran), have been characterized, and their photochromic properties have been fully investigated.

2. RESULTS AND DISCUSSION

2.1. Synthesis and Characterization. Recently, some of us have described new organo-silyl[14] and organo-stannyl[15] POT-based hybrid platforms enabling the covalent attachment of organic ligands using Sonogashira couplings. Among others, two Keggin precursors were obtained. In $(TBA)_3[PW_{11}O_{40}\{Si(C_6H_4I)\}_2]$ (**TBA.K$_{Si}$[I]**, Figure 1a), two $\{Si(C_6H_4I)\}$ groups are connected to the monovacant $\{PW_{11}\}$ POT, whereas, in $(TBA)_4[PW_{11}O_{39}\{Sn(C_6H_4I)\}]$ (**TBA.K$_{Sn}$[I]**, Figure 1b), one $\{Sn(C_6H_4I)\}$ fragment is inserted into the POT. These two complexes, which then can be covalently bonded to one or two organic fragments, respectively, have been chosen for connecting spiropyran entities. This necessitated the use of SP molecules bearing an alkyne arm. To the best of our knowledge, it is only very recently that the first alkyne/SP compound has been reported (**SPR**, Figure 1c).[16] Considering that this species is not photochromic in the solid state at room temperature, it has thus been selected for our study. In addition, the related benzospiropyran **BSPR** represented in Figure 1d has been synthesized in order to determine if small structural variations of the organic fragment can have significant influences on the optical properties of the targeted materials. Although this spiropyran has not been previously reported, the relevant benzoindolenium precursor has already been characterized,[17] allowing readily synthesizing **BSPR** by reacting it with 2-hydroxy-5-nitrobenzaldehyde. However, ^{1}H NMR spectroscopy revealed that, despite numerous efforts for purifying the crude spiropyran or by modifying the synthetic protocol, **BSPR** is obtained as a mixture, with ca. 10%, estimated by ^{1}H NMR, of a secondary product. Single crystals of the mixture (Supporting Information, Table S1) have been obtained, and X-ray diffraction measurements revealed that the impurity is the bromopropenyl spiropyran derivative **BrBSPR** (see the Supporting Information, Figure S1). Noticeably, the presence

dx.doi.org/10.1021/ic401380a | Inorg. Chem. 2013, 52, 11156−11163

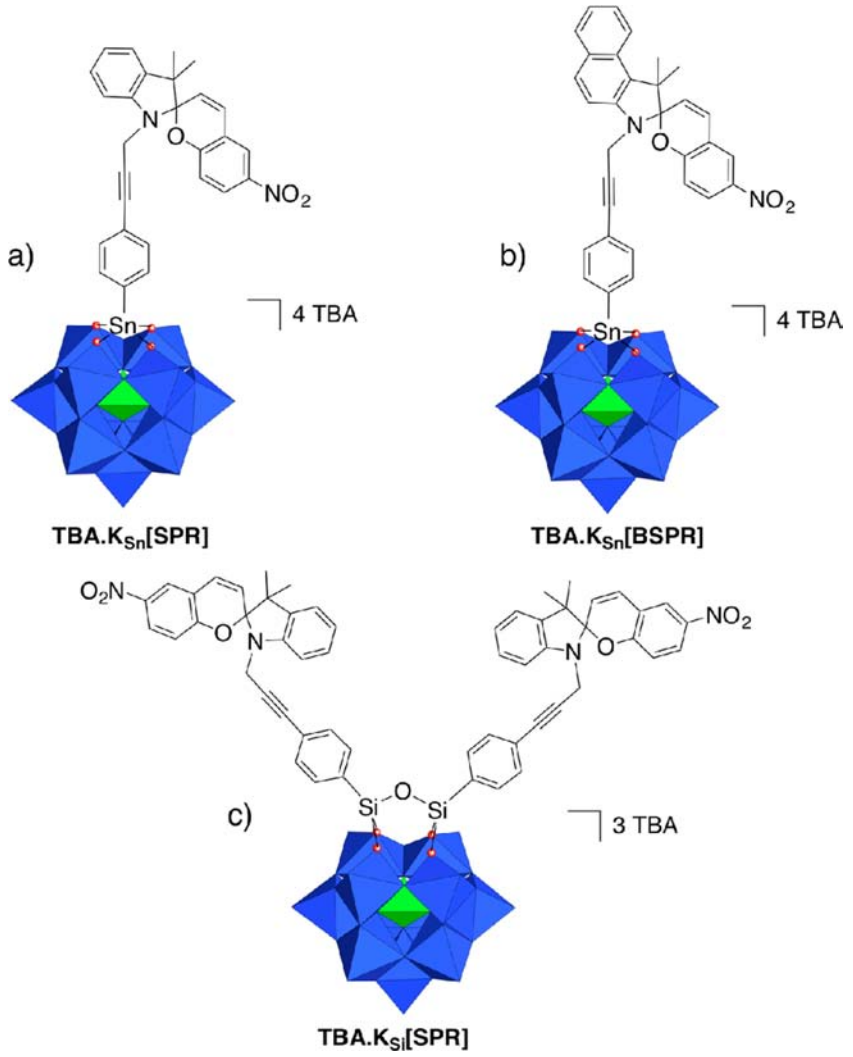

Figure 2. Representation of the three hybrid spiropyran/polyoxotungstates: (a) **TBA.K$_{Sn}$[SPR]**, (b) **TBA.K$_{Sn}$[BSPR]**, and (c) **TBA.K$_{Si}$[SPR]**.

of a small amount of such **BrBSPR** impurities in **BSPR** does not prevent its further use, as the Sonogashira reaction is only effective with alkyne groups.

The coupling between **SPR** and **TBA.K$_{Sn}$[I]** or **TBA.K$_{Si}$[I]**, using a slight excess of spiropyran and under classical conditions (room temperature, 8% $Pd(PPh_3)_2Cl_2$/CuI, DMF, triethylamine), afforded the targeted materials $(TBA)_4[PW_{11}O_{39}\{Sn(C_6H_4(SPR))\}]$ (**TBA.K$_{Sn}$[SPR]**, Figure 2a) and $(TBA)_3[PW_{11}O_{39}\{Si(C_6H_4(SPR))\}_2]$ (**TBA.K$_{Si}$[SPR]**, Figure 2c), respectively. In analogous conditions but using **BSPR**, the compound $(TBA)_4[PW_{11}O_{39}\{Sn(C_6H_4(BSPR))\}]$ (**TBA.K$_{Sn}$[BSPR]**, Figure 2b) has been also obtained. These three species were purified by successive selective precipitations and the use of ion-exchange and exclusion size chromatography. Attempts to isolate single crystals suitable for X-ray diffraction analysis were unsuccessful. However, the purity of the samples was assessed, via ^{1}H and ^{31}P NMR spectroscopy (Supporting Information, Figures S2−S4), elemental analysis, and electrospray ionization mass spectrometry experiments. For all of them, X−C_6H_4−C≡C−CH_2− (X = Si, Sn) groups ensure the connection between the Keggin unit and the SP molecule(s). To further confirm the composition of these hybrid species and to evaluate their electronic properties, electrochemical measurements have also been performed.

The cyclovoltammograms (CVs) of **SPR**, **BSPR**, **TBA.K$_{Sn}$[I]**, **TBA.K$_{Si}$[I]**, **TBA.K$_{Sn}$[SPR]**, **TBA.K$_{Sn}$[BSPR]**, and **TBA.K$_{Si}$[SPR]** are represented in Figure 3. In the +1.00 to −1.80 V/SCE range, the **SPR** and **BSPR** species exhibit only one reversible monoelectronic reduction wave located at $E_{1/2}$ = −1.19 and −1.18 V/SCE, respectively. Considering preceding electrochemical studies devoted to nitrospiropyrans, it can be proposed that this process does not involve the formation of merocyanin and that the extra electron is essentially located on the nitrobenzene moiety, with the formation of a radical anion.[18] Concerning the POT precursors, they display different electron acceptor properties according to the nature of the chemical anchorage (organosilyl vs organotin). Typically, the organosilyl POT derivatives are easier to reduce than the organotin ones, due to the one-charge difference. Indeed, the CVs of **TBA.K$_{Sn}$[I]** and **TBA.K$_{Si}$[I]** exhibit two reversible one-electron waves ($E_{1/2}$ = −1.11 and −1.64 V/SCE) and three reversible one-electron waves ($E_{1/2}$ = −0.37, −1.01, and −1.66 V/SCE), respectively, corresponding to successive redox processes centered on the polyoxotungstate frameworks. Turning now to **TBA.K$_{Sn}$[SPR]**, two reversible waves are observed at $E_{1/2}$ = −1.14 and −1.61 V/SCE, with respective intensities of 2:1. This is thus in perfect agreement with the structure of **TBA.K$_{Sn}$[SPR]**, considering that the waves

dx.doi.org/10.1021/ic401380a | *Inorg. Chem.* 2013, 52, 11156−11163

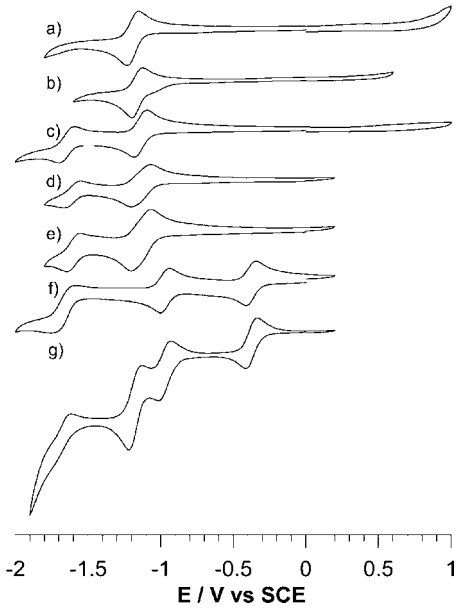

Figure 3. Cyclic voltammograms of 10^{-3} mol·L^{-1} solutions of **SPR** (a), **BSPR** (b), **TBA.K$_{Sn}$[I]** (c), **TBA.K$_{Sn}$[SPR]** (d), **TBA.K$_{Sn}$[BSPR]** (e), **TBA.K$_{Si}$[I]** (f), and **TBA.K$_{Si}$[SPR]** (g) in DMF with 0.1 M $TBAPF_6$ as electrolyte. The scan rate was 100 mV·s^{-1}, and the reference electrode was a saturated calomel electrode (SCE).

observed at $E_{1/2}$ = −1.19 V/SCE for **SPR** and at $E_{1/2}$ = −1.11 V/SCE for **TBA.K$_{Sn}$[I]** are merging in **TBA.K$_{Sn}$[SPR]**. Exactly the same considerations can be made concerning the **TBA.K$_{Sn}$[BSPR]** compound ($E_{1/2}$ = −1.13 and −1.61 V/SCE). Finally, four redox processes are observed for **TBA.K$_{Si}$[SPR]** ($E_{1/2}$ = −0.37, −0.98, −1.18, and −1.66 V/SCE, with relative intensities 1:2:1:1). Again, the waves centered on the POT fragment superimpose with that of the spiropyran and the POT precursors, and confirm the 2:1 SP/POT ratio in **TBA.K$_{Si}$[SPR]**. Overall, these electrochemical measurements are thus confirming the nature of all the reported compounds and indicate that the POT and SP are minimally coupled electronically, as previously observed for organosilyl and organotin POT-based hybrids bonded to neutral organic moieties.[19]

2.2. Optical Properties. The photochromic properties of the reported materials have been studied both in solution and in the solid state. As the MC form is unstable in acetonitrile at room temperature for all of these compounds, the photogeneration of the MC form in solution has systematically been performed at −20 °C. Under UV irradiation (365 nm, 6 W), colorless solutions of **TBA.K$_{Si}$[SPR]** and **TBA.K$_{Sn}$[SPR]** in acetonitrile quickly shift to purple. As shown in Figure 4, the color change of **TBA.K$_{Sn}$[SPR]** is consistent with the appearance of the MC form that is characterized by two absorption bands in the visible region, the first one at λ_{max} around 390 nm, and the second very intense one at λ_{max} = 570 nm. By comparison, this latter arises at λ_{max} = 563 nm for the irradiated **SPR** solution (Supporting Information, Figure S5). These results clearly show that the grafting of SPs on POT platforms does not significantly alter the optical signature of the organic moieties in solution except for a very slight bathochromic effect. The kinetics of the MC → CS thermal ring closure were determined in the dark by following the absorbance of the MC intense absorption as a function of time after irradiating the acetonitrile solutions under 365 nm

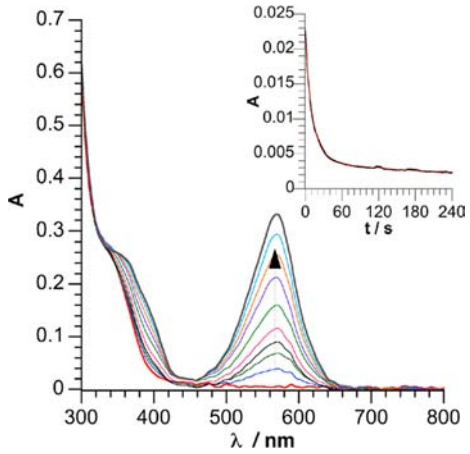

Figure 4. Abs(t) vs t plots for **TBA.K$_{Sn}$[SPR]** in acetonitrile (T = −20 °C, [**TBA.K$_{Sn}$[SPR]**] = 3.10^{-5} mol·L^{-1}) after 0, 5, 10, 15, 20, 30, 45, 60, 75, and 90 min of irradiation at 365 nm. Inset: decay of the Abs(t) vs t plot at λ = 570 nm for **TBA.K$_{Sn}$[SPR]** in acetonitrile (T = 20 °C, [**TBA.K$_{Sn}$[SPR]**] = 3.10^{-5} mol·L^{-1}).

UV irradiation for 5 min at 20 °C. For all compounds, it was found that the Abs(t) vs t curves can only be fitted using a double exponential model (see the Supporting Information, Table S3, for the quantification of the kinetics constants), a single exponential model being not suitable (Supporting Information, Figure S6). Such a phenomenon has already been observed for many SPs, a plausible explanation being the existence of different isomers of the MC form in solution.[20] It can also be proposed that, in these compounds, the slowest process (related to k_2) is linked to the isomerization process and the quickest one (related to k_1) to the ring closure. Interestingly, it can be noted that, whereas k_1 is only slightly affected when the SP is grafted on the POT platform, the formation of a hybrid material has a significant influence on the k_2 constant.

The solid-state photochromic properties of the three hybrid SP−POT materials have been investigated in ambient conditions by diffuse reflectance spectroscopy of microcrystalline powders. **TBA.K$_{Sn}$[SPR]**, **TBA.K$_{Sn}$[BSPR]**, and **TBA.K$_{Si}$[SPR]** have an optical gap at 423, 410, and 414 nm, respectively (Supporting Information, Figure S7). By comparison, the optical gap of $(TBA)_4H_3[PW_{11}O_{39}]$—a POT reference that does not contain spiropyran moieties—arises at a higher energy (342 nm). This shows that the SP moiety dictates the absorption threshold in the three hybrid compounds, similarly as in the SP−$\{MnMo_6O_{18}\}$ dyads.[12] Very importantly, whereas **SPR** is nonphotochromic in the solid state in ambient conditions, the beige powder of **TBA.K$_{Sn}$[SPR]** (Figure 5a) gradually shifts to deep purple under low-power UV excitation (365 nm, 6 W). The photochromic effect, which is detectable with the naked eye after only 3 s, does not evolve anymore after 20 min, revealing a very fast photoresponse and a strong coloration contrast. As observed in solution, the color change is associated with the growth of the two absorptions characteristic of the MC form with the more intense one located at λ_{max} = 584 nm (Figure 5b). Under similar UV exposure, the powder of **TBA.K$_{Si}$[SPR]** develops the same purple coloration, the maximum of the intense photogenerated MC absorption band being also located at 584 nm (Supporting Information, Figure S8), however, with a color change less pronounced than that for **TBA.K$_{Sn}$[SPR]**. In marked

dx.doi.org/10.1021/ic401380a | Inorg. Chem. 2013, 52, 11156−11163

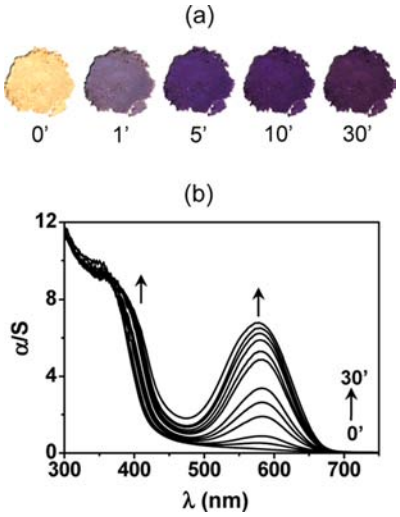

Figure 5. (a) Photographs of powders of **TBA.K$_{Sn}$[SPR]** after different 365 nm UV irradiation times (in min). (b) Evolution of the photogenerated absorption in **TBA.K$_{Sn}$[SPR]** after 0, 0.166, 0.5, 1, 1.5, 2, 3, 4, 5, 8, 15, and 30 min of UV irradiation (365 nm).

contrast with **TBA.K$_{Sn}$[SPR]**, **TBA.K$_{Sn}$[BSPR]** does not display any significant solid-state photochromic activity in ambient conditions (Supporting Information, Figure S9), the color change remaining quasi undetectable by human eyes even after irradiating the powdered sample under UV excitation for a period as long as 1 day. This result underlines that small structural variations of the SP moieties can induce dramatic damages in the optical properties of the hybrid SP–POT materials. Nevertheless, **TBA.K$_{Si}$[SPR]** and **TBA.K$_{Sn}$[SPR]** clearly illustrate that the grafting of SP molecules—initially nonphotochromic in the solid state—onto POT fragments is a powerfull strategy to reach solid materials with strong photoresponses.

The coloration kinetics of powders of **TBA.K$_{Sn}$[SPR]** and **TBA.K$_{Si}$[SPR]** at room temperature have been quantified from the evolution of the photogenerated MC absorption with the 365 nm UV irradiation time t (Supporting Information, Figure S10), and details of the kinetics parameters are given in the Supporting Information (Table S4). Because of its very weak photoresponse, the coloration kinetics of **TBA.K$_{Sn}$[BSPR]** has not been investigated. Figure 6 displays the absorption at λ_{max} = 584 nm ($Abs^{584}(t)$) as a function of the UV irradiation time t

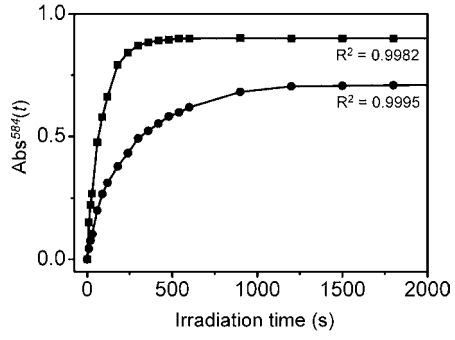

Figure 6. $Abs^{584}(t)$ vs t plots for **TBA.K$_{Sn}$[SPR]** (■) and **TBA.K$_{Si}$[SPR]** (●). The lines show the fits of the plots according to rate laws $Abs^{584}(t) = A_1(\exp(-k_1t) - 1)$ and $Abs^{584}(t) = -A_1 - A_2 + A_1\exp(-k_1t) + A_2\exp(-k_2t)$ for **TBA.K$_{Sn}$[SPR]** and **TBA.K$_{Si}$[SPR]**, respectively (R^2 are the regression coefficients for the fits).

for **TBA.K$_{Sn}$[SPR]** and **TBA.K$_{Si}$[SPR]**. It is worth noting that **TBA.K$_{Sn}$[SPR]** shows a very fast and intense color change effect, and the $Abs^{584}(t)$ vs t plot can be well-fitted by a single-exponential rate law, with the coloration rate constant k^c_1 = 0.012 s^{-1}. In the case of **TBA.K$_{Si}$[SPR]**, the coloration rate significantly deviates from first-order kinetics but can be adequately fitted using a biexponential rate law with k^c_1 = 0.003 s^{-1} and k^c_2 = 0.018 s^{-1}, k^c_1 describing the major contribution (around 77%) of the temporal evolution of $Abs^{584}(t)$. This could be tentatively explained considering that (i) two SP molecules are grafted onto the POT unit in **TBA.K$_{Si}$[SPR]** (for only one in the case of **TBA.K$_{Sn}$[SPR]**), both of them contributing to the global absorption in the visible, and (ii) the two MC open forms could be localized in different environments in the framework. As expected from photographs, the photocoloration response of **TBA.K$_{Si}$[SPR]** is slower and less intense, despite the two SP units, than for **TBA.K$_{Sn}$[SPR]**, signifying at first sight that, in ambient conditions, the CS → MC photoinduced switch could be less effective in **TBA.K$_{Si}$[SPR]** than in **TBA.K$_{Sn}$[SPR]**.

The color fading rates of **TBA.K$_{Sn}$[SPR]** and **TBA.K$_{Si}$[SPR]** in the solid state were measured in the dark (thermal fading) and under yellow light, at room temperature, by monitoring the temporal decay of the absorption band located at λ_{max} = 584 nm of samples once irradiated under UV excitation for 30 min (Supporting Information, Figures S11 and S12). Decays can be well-fitted using a biexponential rate law (see the Supporting Information, Table S4, for detailed fading kinetic parameters). As already proposed for other spiro-derivatives,[21] this could be interpreted as the result of two different structural micro-environments around the merocyanin forms photogenerated at the surface of the samples or lying deeper inside the bulk (let us underline that the UV irradiation does not affect all the bulk of the samples but is only limited to a small volume under the surface, which depends on the penetration depth of the UV light in the materials). During the thermal fading process, the absorption of both materials exhibits a loss of only about 20% in intensity, showing that, in the dark, a large part of the UV-photogenerated zwitterionic MC form remains stabilized in the polar hybrid framework. The extracted thermal fading rate constants are k^f_1 = 1.426 .10^{-4} s^{-1} and k^f_2 = 0.024 s^{-1} for **TBA.K$_{Sn}$[SPR]**, and k^f_1 = 2.282 .10^{-4} s^{-1} and k^f_2 = 0.029 s^{-1} for **TBA.K$_{Si}$[SPR]** (in each case, k^f_1 describes the major contribution of the temporal evolution of the absorption). For each system, the significant difference in kinetic constant values k^f_1 and k^f_2 and in the amplitudes (A_1 and A_2) extracted from the fits could be explained considering at first sight that the majority of the zwitterionic MC forms are photogenerated near the surface while a smaller amount is generated deeper in the bulk. A specific MC molecule near the surface is mostly surrounded by similar open forms. Thus, the polarity of its local environment increases and the MC molecule is better stabilized. Therefore, the MC → CS thermal back conversion (related to k^f_1) should be slow. At the opposite, MC forms in the bulk are mainly surrounded by less polar CS isomers, and so, they should be less stabilized in the framework. Hence, the associated thermal MC → CS isomerization (related to k^f_2) should be strongly faster. These values are quite comparable with those of other hybrid materials based on spiropyran molecules embedded in silica-gel matrixes,[22] and they are much faster than those of the rarest pure spiropyran molecules developing solid-state photochromism at room temperature.[3a,23] Interestingly, the color fading process at room

dx.doi.org/10.1021/ic401380a | Inorg. Chem. 2013, 52, 11156–11163

temperature is considerably accelerated when the irradiated samples are put under yellow light, that is, with energy corresponding to that of the photogenerated absorption.[2] The absorption loss is about 75% for both materials, and the color fading rates are more than 3 times faster than in the dark (k^f_1 = 5.056 .10^{-4} s^{-1} and k^f_2 = 0.076 s^{-1} for **TBA.K$_{Sn}$[SPR]**, and k^f_1 = 7.434 .10^{-4} s^{-1} and k^f_2 = 0.035 s^{-1} for **TBA.K$_{Si}$[SPR]**).

3. CONCLUSION

We have thus reported here the first examples of compounds based on the covalent association of polyoxotungstates and organic photochromic molecules. The synthetic approach used here—based on Sonogashira couplings—allowed us to easily modulate the nature of the inorganic platform (redox properties and number of grafted organic molecules), and the organic chromophore. The purity of all the synthesized complexes has been unambiguously assessed using multiple physical techniques, and their optical properties have been deeply investigated. In solution, it has been observed that the polyoxotungstate core does not significantly alter the optical signature of the organic moieties but affects the kinetics of the MC→ CS thermal ring formation. Furthermore, in the solid state, it is shown that the grafting of a POT on a nonphotochromic organic fragment can lead to highly photochromic molecular hybrid compounds. However, this observation cannot be generalized, and it has been found that very slight topological modifications can strongly influence the solid-state photochromic properties of these new molecular systems. Exploitation of the dual electrochromic and photochromic properties of these hybrids is under current investigation. We are also exploring emerging luminescence properties arising from the covalent combination of such organic and inorganic components. The results of these studies will be reported soon.

4. EXPERIMENTAL SECTION

4.1. Methods and Materials. Solvents, including triethylamine, were dried over suitable reagents and freshly distilled under argon before use. The reagents 1-tosyl-2-propyne,[16] $K_7[PW_{11}O_{39}]\cdot 14H_2O$,[24] $[Pd(PPh_3)_2Cl_2]$,[25] 1-iodo-4-(triethoxysilyl)benzene,[26] 1-iodo-4-(trichlorotin)benzene,[15] **TBA.K$_{Sn}$[I]**,[15] and **TBA.K$_{Si}$[I]**[14b] were synthesized according to published procedures. The ^{1}H (300.13 MHz, 400.13 MHz), and $\{^1H\}$ ^{31}P (162 MHz) NMR spectra were obtained at room temperature in 5 mm o.d. tubes on a Bruker Avance II 300 or Bruker Avance III 400 spectrometer equipped with a QNP probe head. IR spectra were recorded from KBr pellets using a Biorad FT 165 spectrometer. Elemental analyses were performed at the Institut des Substances Naturelles, Gif sur Yvette, France. Cyclic voltammetry experiments at a carbon electrode were carried out using the EG&G model 273A system. A standard three-electrode cell was used, which consisted of a working vitrous carbon electrode, an auxiliary platinum electrode, and an aqueous saturated calomel electrode (SCE) equipped with a double junction.

4.2. X-ray Crystal Structure Determination of BrBSP. A single crystal of compound **BrBSP** was selected, mounted onto a glass fiber, and transferred under a cold nitrogen gas stream. Intensity data were collected with a Bruker Kappa APEX2 with graphite monochromated Mo Kα radiation. Unit cell parameter determination, data collection strategy, and integration were carried out with the APEX 2 suite of programs. Multiscan absorption correction was applied.[27] The structure was solved by direct methods with SHELXL software.[28] All nonhydrogen atoms were refined anisotropically. All hydrogen atoms were placed at calculated positions. The crystallographic data and refinement parameters for **BrBSP** are summarized in Table S1 (Supporting Information). The crystallographic details are available in the Supporting Information in CIF format. CCDC no. 940802. These data can be obtained free of charge from the Cambridge Crystallographic Data Centre via www.ccdc.cam.ac.uk/data_request/cif.

4.3. Optical Measurements. Diffuse reflectance spectra were collected at room temperature on a finely ground sample with a Cary 5G spectrometer (Varian) equipped with a 60 mm diameter integrating sphere and computer-controlled using the "Scan" software. Diffuse reflectance was measured from 250 to 1550 nm with a 2 nm step using Halon powder (from Varian) as reference (100% reflectance). The reflectance data were treated by a Kubelka–Munk transformation[29] to better locate the absorption thresholds. The samples were irradiated with a Fisher Bioblock labosi UV lamp (λ_{exc} = 365 nm, P = 6 W). The photocoloration and fading kinetics were quantified by monitoring the temporal evolution of the absorption Abs(t), which was defined as Abs(t) = −log($R(t)/R(0)$), with $R(t)$ and $R(0)$ the reflectivity at the time t and at t = 0, respectively.

4.4. Syntheses of the Compounds. *4.4.1. Synthesis of 1,3-Dihydro-3,3-dimethyl-1-propargyl-6-nitrospiro[2H-1-benzopyran-2,2-(2H)-indole] (**SPR**).* This compound has been synthesized by a slight modification of the literature procedure.[16] 2,3,3-Trimethyl indolenine (2.000 g, 12.6 mmol) and 2-propyn-1-tosyl (3.957 g, 18.9 mmol) were heated overnight at 70 °C. After cooling down to room temperature, CH_2Cl_2 (10 mL) was added to the purple mixture and the solution was extracted with water (20 mL). The aqueous phase was then washed with $CHCl_3$ (10 mL) three times and evaporated to dryness, yielding a green oil that was dissolved in 2-butanone (40 mL). Piperidin (0.623 g, 7.3 mmol), followed by 2-hydroxy-5-nitrobenzaldehyde (1.219 g, 7.3 mmol), were then added. The resulting dark red suspension was heated under reflux (90 °C) for 3 h, cooled down to room temperature, and then stirred for 15 h. The obtained suspension was filtered, and the precipitate was washed with 2-butanone (2 × 3 mL). The filtrate was evaporated and purified through silica gel chromatography (eluent CH_2Cl_2) to yield an orange sticky solid (633 mg; yield: 15%). ^{1}H NMR, 300 MHz, $CDCl_3$: δ 8.04 (dd, J = 9.8, 2.7 Hz, 1H), 8.02 (d, J = 2.6 Hz, 1H), 7.22 (dd, J = 7.60, 1.4 Hz, 1H), 7.13 (dd, J = 7.2, 1.0 Hz, 1H), 7.00 (d, J = 10.4 Hz, 1H), 6.95 (dt, J = 7.6, 7.25, 0.9 Hz, 1H), 6.83 (d, J = 7.8 Hz, 1H,), 6.65 (d, J = 9.8 Hz, 1H), 5.89 (d, J = 10.4 Hz, 1H), 4.07 (dd, J = 18.1, 2.6 Hz, 1H), 3.85 (dd, J = 18.1, 2.4 Hz, 1 H), 2.10 (t, J = 2.5 Hz, 1H), 1.31 (s, 3H), 1.21 (s, 3H).

*4.4.2. Synthesis of 1,3-Dihydro-3,3-dimethyl-1-propargyl-6-nitrospiro[2H-1-benzopyran-2,2-(2H)-(1H)benzindole] (**BSPR**).* 1,1,2-Trimethyl-1*H*-benzindolenine (2 g, 9.6 mmol) and propargyl bromide (1.7 g, 14.3 mmol) were suspended in acetonitrile (10 mL) and heated at reflux for 24 h. The resulting dark blue solution was then cooled down to room temperature and evaporated. After addition of CH_2Cl_2 (10 mL), the solution was extracted with water (20 mL). The red aqueous solution was then washed with CH_2Cl_2 (10 mL) and $CHCl_3$ (2 × 10 mL). The evaporation of the aqueous phase yielded a red oil to which was added 2-butanone (7 mL), piperidin (144 mg, 1.69 mmol), and 2-hydroxy-5-nitrobenzaldehyde (283 mg, 1.69 mmol). The resulting dark red suspension was heated under reflux (90 °C) for 3 h, cooled down to room temperature, and then stirred for 15 h. The suspension was filtered, and the solid was washed with cold 2-butanone (2 × 3 mL). The filtrate was evaporated and purified through silica gel chromatography (eluent CH_2Cl_2) to yield 141 mg of a powder of **BSPR** with ca. 10% of 1,3-dihydro-3,3-dimethyl-1-(3-bromoprop-2-enyl)-6-nitrospiro[2*H*-1-benzopyran-2,2-(2*H*)-(1*H*)-benzindole] (**BrBSPR**) as an impurity. ^{1}H NMR, 300 MHz, $CDCl_3$: δ 8.05−7.80 (m, 5H), 7.45 (td, 1H), 7.30 (m, 1H), 7.22 (m, 1H), 7.03 (d, J = 10.4 Hz, 1H), 6.71 (d, J = 10.2 Hz, 1H), 5.96 (d, J = 10.40 Hz, 1H), 4.16 (dd, 1H, J = 18.2, 2.6 Hz, 1H), 3.95 (dd, J = 18.22, 2.50 Hz, 1H), 2.11 (t, J = 2.50 Hz, 1H), 1.66 (s, 3H), 1.39 (s, 3H).

*4.4.3. Synthesis of **TBA.K$_{Sn}$[SPR]**.* In a dried Schlenk flask, **SPR** (34.6 mg, 0.1 mmol), $TBA_4[PW_{11}O_{39}\{SnPhI\}]$ (200 mg, 0.05 mmol), $Pd(PPh_3)_2(Cl)_2$ (2.3 mg, 0.004 mmol), and CuI (0.8 mg, 0.004 mmol) were dissolved in 4 mL of dry DMF under an argon atmosphere. Freshly distilled triethylamine (0.14 mL, 1 mmol) was then added, and the mixture was stirred for 24 h. The resulting dark red solution was precipitated with diethyl ether (150 mL), and the orange precipitate was filtered, redissolved in acetonitrile (10 mL), and stirred with 5 mL

dx.doi.org/10.1021/ic401380a | Inorg. Chem. 2013, 52, 11156−11163

of Amberlite IR-120 in the TBA^+ form. The resulting orange solution was then precipitated and dried with diethyl ether, yielding an orange powder (180 mg, Yield: 86%). ^{1}H NMR, 400 MHz, CD_3CN: δ 8.12 (d, J = 2.8 Hz, 1H), 8.01 (dd, J = 9.0, 2.8 Hz, 1H), 7.61 (d + dd, J = 8.2 Hz, J_{SnH} = 96.0 Hz, 2H), 7.32 (d+ dd, J = 8.2 Hz, J_{SnH} = 33.0 Hz, 2H), 7.23 (td, J = 7.7, 1.3 Hz, 1H), 7.18 (ddd, J = 7.7, 1.3, 0.6 Hz, 1H), 7.15 (dd, J = 10.4, 0.7 Hz, 1H), 6.92 (td, J = 7.7, 1.3 Hz, 1H), 6.87 (dt, J = 7.7, 0.7 Hz, 1H), 6.74 (dd, J = 9.0, 0.7 Hz, 1H), 6.00 (d, J = 10.4 Hz, 1H), 4.36 (d, J = 18.4 Hz, 1H), 4.17 (d, J = 18.4 Hz, 1H), 3.15 (m, 32H), 1.64 (m, 32H), 1.38 (sextuplet, J = 7.3 Hz, 32H), 1.31 (s, 3H), 1.19 (s, 3H), 0.97 (t, J = 7.3 Hz, 48H). ^{31}P NMR, 162 MHz, CD_3CN: δ −10.99 (s + d, J_{SnP} = 23.5 Hz). IR (KBr, cm^{-1}): ν 2962 (m), 2933 (m), 2873 (m), 2360 (w), 2340 (w), 1652 (w), 1519 (w), 1482 (m), 1459 (m), 1380 (w), 1337 (w), 1276 (w), 1070 (m), 963 (s), 886 (s), 811 (s), 706 (w), 667 (w), 593 (w), 514 (w), 381 (m), 336 (w), 302 (w), 265 (m). MS (ESI): most intense peaks, {Aggregates}$^{x-}$ m/z $\{[K_{Sn}[SP]]\}^{4-}$ 804.8 (100), calcd 804.8; $\{H[K_{Sn}[SP]]\}^{3-}$ 1072.4 (75), calcd 1072.1; $\{TBA{\cdot}H[K_{Sn}[SP]]\}^{2-}$ 1730.4 (25), calcd 1730.3. Anal. Calcd for $PW_{11}SnO_{42}C_{27}H_{21}N_2C_{64}H_{144}N_4(H_2O)_2$: C, 25.88; H, 4.03; N, 1.99. Found: C, 25.65; H, 3.95; N, 2.05.

4.4.4. Synthesis of ***TBA.K$_{Sn}$[BSPR]$$.*** This compound was obtained following the same experimental protocol than that described for **TBA.K$_{Sn}$[SPR]**, using the raw **BSPR** compound (36.9 mg, 0.1 mmol) instead of the **SPR** one, as an orange powder (174 mg, Yield: 82%). ^{1}H NMR, 400 MHz, CD_3CN: δ 8.14 (d, J = 2.8 Hz, 1H), 8.06 − 7.97 (m, 2H), 7.92−7.83 (m, 2H), 7.60 (d + dd, J = 8.2 Hz, J_{SnH} = 96.0 Hz, 2H), 7.46 (ddd, J = 8.3, 6.8, 1.3 Hz, 1H), 7.38−7.29 (m, 3H), 7.29 (ddd, J = 8.3, 6.8, 1.1 Hz, 1H), 7.21 (dd, J = 10.4, 0.7 Hz, 1H), 6.72 (dd, J = 9.1, 0.6 Hz, 1H), 6.08 (d, J = 10.4 Hz, 1H), 4.48 (d, J = 18.6 Hz, 1H), 4.26 (d, J = 18.6 Hz, 1H). 3.15 (m, 32H), 1.65 (s, 3H), 1.64 (m, 32H), 1.38 (sextuplet, J = 7.3 Hz, 32H), 1.36 (s, 3H), 0.97 (t, J = 7.3 Hz, 48H). ^{31}P NMR, 162 MHz, CD_3CN: δ = −10.99 (s + d, J_{SnP} = 24.3 Hz). IR (KBr, cm^{-1}): ν 2962 (m), 2934 (m), 2873 (m), 2360 (w), 2340(w), 1623 (w), 1519 (w), 1482 (m), 1380 (w), 1336 (m), 1279 (w), 1069 (s), 963 (s), 886 (s), 813 (s), 705 (w), 667 (w), 593 (w), 514 (w), 381 (m), 334 (w), 265 (m). MS (ESI): most intense peaks, {Aggregates}$^{x-}$ m/z (%):$\{H[K_{Sn}[BSP]]\}^{3-}$ 1089.4 (100), calcd 1089.4; $\{TBA{\cdot}H[K_{Sn}[BSP]]\}^{2-}$ 1754.3 (40), calcd 1754.3. Anal. Calcd for $C_{95}H_{167}N_6O_{42}PSnW_{11}$: C, 26.93; H, 3.97; N, 1.98. Found: C, 27.41; H, 3.96; N, 2.08.

4.4.5. Synthesis of ***TBA.K$_{Si}$[SPR]$$.*** In a dried Schlenk flask, **SPR** (70.6 mg, 0.204 mmol), $TBA_3[PW_{11}O_{40}\{SiPhI\}_2]$ (200 mg, 0.05 mmol), $Pd(PPh_3)_2(Cl)_2$ (2.9 mg, 0.004 mmol), and CuI (0.8 mg, 0.004 mmol) were dissolved under argon in 4 mL of dry DMF. Freshly distilled triethylamine (0.15 mL, 1 mmol) was then added, and the reaction was stirred for 24 h. Diethyl ether (150 mL) was added to the dark green solution, and the precipitate was filtered. The dark green solid was then redissolved in acetonitrile (50 mL), and the resulting solution was stirred for 30 min and then evaporated to dryness. After redissolution in CH_2Cl_2, TBABr was added in excess. The product was purified via an LH20 column in CH_2Cl_2. The filtrate was then precipitated with diethyl ether, yielding an orange powder after filtration (130 mg, Yield: 62%). ^{1}H NMR, 400 MHz, CD_3CN: δ 8.11 (d, J = 2.9 Hz, 2H), 8.02−7.94 (m, 1H), 7.73 (d, J = 8.2 Hz, 4H), 7.32 (d, J = 8.2 Hz, 4H), 7.22 (td, J = 7.7, 1.3 Hz, 2H), 7.17 (ddd, J = 7.7, 1.3, 0.6 Hz, 2H), 7.13 (dd, J = 10.4, 0.5 Hz, 2H), 6.91 (td, J = 7.7, 1.3 Hz, 2H), 6.88 (d, J = 7.7 Hz, 2H), 6.72 (dd, J = 9.0, 0.7 Hz, 2H), 6.00 (d, J = 10.4 Hz, 2H), 4.36 (d, J = 18.5 Hz, 2H), 4.16 (d, J = 18.5 Hz, 2H), 3.12 (m, 24H), 1.63 (m, 24H), 1.37 (sextuplet, J = 7.4 Hz, 24H), 1.30 (s, 3H), 1.18 (s, 3H), 0.97 (t, J = 7.4 Hz, 32 H). ^{31}P NMR, 162 MHz, CD_3CN: δ −12.13 (s). IR (KBr, cm^{-1}): ν 2963 (m), 2933 (m), 2874 (m), 2360 (w), 2340 (w), 1609 (w), 1519 (w), 1482 (m), 1458 (w), 1380 (w), 1337 (m), 1275 (w), 1160 (w), 1110 (m), 1090 (w), 1067 (m), 1039 (m), 965 (s), 872 (s), 824 (s), 769 (m), 748 (m), 716 (w), 668 (w), 589 (m), 521 (m), 394 (m), 353 (w), 278 (m). MS (ESI): Most intense peaks, {Aggregates}$^{x-}$ m/z (%): $\{[K_{Si}[SP]]\}^{3-}$ 1197.5 (100), calcd 1197.5; $\{TBA[K_{Si}[SP]]\}^{2-}$ 1917.3 (20), calcd 1916.4. Anal. Calcd for $PW_{11}Si_2O_{46}C_{54}H_{42}N_4C_{48}H_{108}N_3$: C, 28.36; H, 3.50; N, 2.27. Found: C, 28.48; H, 3.50; N, 2.10.

■ ASSOCIATED CONTENT

Ⓢ Supporting Information

Tables containing crystallographic data, half-wave potentials, kinetic parameters, and coloration and fading kinetic parameters and figures showing structural representations, ^{1}H and ^{31}P NMR spectra, Abs(t) vs t plots, double and single exponential fits, Kubelka−Munk transformed reflectivity vs wavelength and energy plots, photographs of powders, evolution of the photogenerated absorption, and temporal evolution of the absorbance at 584 nm. This material is available free of charge via the Internet at http://pubs.acs.org.

■ AUTHOR INFORMATION

Corresponding Authors

*E-mail: guillaume.izzet@upmc.fr.
*E-mail: remi.dessapt@cnrs-imn.fr.
*E-mail: pierre.mialane@uvsq.fr.

Notes

The authors declare no competing financial interest.

■ ACKNOWLEDGMENTS

We thank the CNRS, the Ministère de l'Enseignement Supérieur et de la Recherche, and the ANR-11-BS07-011-01 BIOOPOM.

■ REFERENCES

(1) Hirshberg, Y.; Fisher, E. *J. Chem. Phys.* **1955**, *23*, 1723.
(2) Natali, M.; Giordani, S. *Chem. Soc. Rev.* **2012**, *41*, 4010.
(3) (a) Bénard, S.; Yu, P. *Adv. Mater.* **2000**, *12*, 48. (b) Godsi, O.; Peskin, U.; Kapon, M.; Natan, E.; Eichen, Y. *Chem. Commun.* **2001**, 2132.
(4) (a) Berkovic, G.; Krongauz, V.; Weiss, V. *Chem. Rev.* **2000**, *100*, 1741. (b) Dürr, H., Bouas-Laurent, H., Eds. *Photochromism: Molecules and Systems*; Elsevier: Amsterdam, 2003. (c) Feringa, B. L., Ed. *Molecular Switches*; Wiley-VCH: Weinheim, 2001.
(5) (a) Wang, M.-S.; Xu, G.; Zhang, Z.-J.; Guo, G.-C. *Chem. Commun.* **2010**, *46*, 361. (b) Pardo, R.; Zayat, M.; Levy, D. *Chem. Soc. Rev.* **2011**, *40*, 672.
(6) (a) Giordani, S.; Raymo, F. M. *Org. Lett.* **2003**, *5*, 3559. (b) Raymo, F. M.; Giordani, S. *J. Am. Chem. Soc.* **2001**, *123*, 4651.
(7) Zhang, F.; Zou, X.; Feng, W.; Zhao, X.; Jing, X.; Sun, F.; Ren, H.; Zhu, G. *J. Mater. Chem.* **2012**, *22*, 25019.
(8) (a) Park, I. S.; Jung, Y.-S.; Lee, K.-J.; Kim, J.-M. *Chem. Commun.* **2010**, *46*, 2859. (b) Wagner, K.; Byrne, R.; Zanoni, M.; Gambhir, S.; Dennany, L.; Breukers, R.; Higgins, M.; Wagner, P.; Diamond, D.; Wallace, G. G.; Officer, D. L. *J. Am. Chem. Soc.* **2011**, *133*, 5453.
(9) Bahr, J. L.; Kodis, G.; de la Garza, L.; Lin, S.; Moore, A. L.; Moore, T. A.; Gust, D. *J. Am. Chem. Soc.* **2001**, *123*, 7124.
(10) (a) Long, D.-L.; Tsunashima, R.; Cronin, L. *Angew. Chem., Int. Ed.* **2010**, *49*, 1736. (b) Bassil, B. S.; Kortz, U. *Z. Anorg. Allg. Chem.* **2010**, *636*, 2222. (c) Lu, H.; Geletii, Y. V.; Zhao, C.; Vickers, J. W.; Zhu, G.; Luo, Z.; Song, J.; Lian, T.; Musaev, D. G.; Hill, C. L. *Chem. Soc. Rev.* **2012**, *41*, 7572. (d) Dolbecq, A.; Dumas, E.; Mayer, C. R.; Mialane, P. *Chem. Rev.* **2010**, *110*, 6009. (e) Dolbecq, A.; Mialane, P.; Sécheresse, F.; Keita, B.; Nadjo, L. *Chem. Commun.* **2012**, *48*, 8299.
(11) (a) Mialane, P.; Zhang, G. J.; Mbomekallé, I. M.; Yu, P.; Compain, J.-D.; Dolbecq, A.; Marrot, J.; Sécheresse, F.; Keita, B.; Nadjo, L. *Chem.—Eur. J.* **2010**, *16*, 5572. (b) Compain, J.-D.; Deniard, P.; Dessapt, R.; Dolbecq, A.; Oms, O.; Sécheresse, F.; Marrot, J.; Mialane, P. *Chem. Commun.* **2010**, *46*, 7733.
(12) Oms, O.; Hakouk, K.; Dessapt, R.; Deniard, P.; Jobic, S.; Dolbecq, A.; Palacin, T.; Nadjo, L.; Keita, B.; Marrot, J.; Mialane, P. *Chem. Commun.* **2012**, *48*, 12103.
(13) (a) Gouzerh, P.; Proust, A. *Chem. Rev.* **1998**, *98*, 77. (b) Proust, A.; Thouvenot, R.; Gouzerh, P. *Chem. Commun.* **2008**, 1837.

(c) Proust, A.; Matt, B.; Villanneau, R.; Guillemot, G.; Gouzerh, P.; Izzet, G. *Chem. Soc. Rev.* **2012**, *41*, 7605.
(14) (a) Duffort, V.; Thouvenot, R.; Afonso, C.; Izzet, G.; Proust, A. *Chem. Commun.* **2009**, 6062. (b) Matt, B.; Renaudineau, S.; Chamoreau, L. M.; Afonso, C.; Izzet, G.; Proust, A. *J. Org. Chem.* **2011**, *76*, 3107.
(15) Matt, B.; Moussa, J.; Chamoreau, L.-M.; Afonso, C.; Proust, A.; Amouri, H.; Izzet, G. *Organometallics* **2011**, *31*, 35.
(16) Bertoldo, M.; Nazzi, S.; Zampano, G.; Ciardelli, F. *Carbohydr. Polym.* **2011**, *85*, 401.
(17) Zhan, W.-H.; Barnhill, H. N.; Sivakumar, K.; Tian, H.; Wang, Q. *Tetrahedron Lett.* **2005**, *46*, 1691.
(18) (a) Zhi, J. F.; Baba, R.; Hashimoto, K.; Fujishima, A. *J. Photochem. Photobiol., A* **1995**, *92*, 91. (b) Campredon, M.; Giusti, G.; Guglielmetti, R.; Samat, A.; Gronchi, G.; Alberti, A.; Benaglia, M. *J. Chem. Soc., Perkin Trans. 2* **1993**, 2089.
(19) (a) Matt, B.; Coudret, C.; Viala, C.; Jouvenot, D.; Loiseau, F.; Izzet, G.; Proust, A. *Inorg. Chem.* **2011**, *50*, 7761. (b) Matt, B.; Xiang, X.; Kaledin, A. L.; Han, N.; Moussa, J.; Amouri, H.; Alves, S.; Hill, C. L.; Lian, T.; Musaev, D. G.; Izzet, G.; Proust, A. *Chem. Sci.* **2013**, *4*, 1737.
(20) (a) Pimienta, V.; Lavabre, D.; Levy, G.; Samat, A.; Guglielmetti, R.; Micheau, J. C. *J. Phys. Chem.* **1996**, *100*, 4485. (b) Wetzler, D. E.; Aramendía, P. F.; Japas, M. L.; Fernández-Prini, R. *Phys. Chem. Chem. Phys.* **1999**, *1*, 4955. (c) Bahr, J. L.; Kodis, G.; de la Garza, L.; Lin, S.; Moore, A. L.; Moore, T. A.; Gust, D. *J. Am. Chem. Soc.* **2001**, *123*, 7124. (d) Grofcsika, A.; Baranyaia, P.; Bitterc, I.; Grünc, A.; Köszegic, E.; Kubinyia, M.; Pála, K.; Vidóczya, T. *J. Mol. Struct.* **2002**, *614*, 69.
(21) Benard, S.; Yu, P. *Chem. Commun.* **2000**, 65.
(22) (a) Schaudel, B.; Guermeur, C.; Sanchez, C.; Nakatani, K.; Delaire, J. A. *J. Mater. Chem* **1997**, *7*, 61. (b) Léaustic, A.; Dupont, A.; Yu, P.; Clément, R. *New. J. Chem.* **2001**, *25*, 1297.
(23) Aldoshin, S. M.; Nikonova, L. A.; Smirnov, V. A.; Shilov, G. V.; Nagaeva, N. K. *J. Mol. Struct.* **2005**, *750*, 158.
(24) Souchay, P. *Polyanions et Polycations*; Gauthier-Villars: Paris, 1963.
(25) Dangles, O.; Guibe, F.; Balavoine, G.; Lavielle, S.; Marquet, A. *J. Org. Chem.* **1987**, *52*, 4984.
(26) Maegawa, Y.; Nagano, T.; Yabuno, T.; Nakagawa, H.; Shimada, T. *Tetrahedron* **2007**, *63*, 11467.
(27) (a) Duisenberg, A. J. M.; Kroon-Batenburg, L. M.; Schreurs, J. A. M. M. *J. Appl. Crystallogr.* **2003**, *36*, 220. (b) Blessing, R. H. *Acta Crystallogr., Sect. A* **1995**, *51*, 33.
(28) (a) Altomare, A.; Cascarano, G.; Giacovazzo, C.; Guagliardi, A.; Burla, M. C.; Polidori, G.; Camalli, M. *J. Appl. Crystallogr.* **1994**, *27*, 435. (b) Palatinus, L.; Chapuis, G. *J. Appl. Crystallogr.* **2007**, *40*, 786. (c) Sheldrick, G. M. *Acta Crystallogr., Sect. A* **2008**, *64*, 112.
(29) Kubelka, P.; Munk, F. *Z. Tech. Phys.* **1931**, *12*, 593.